Phase diagrams and electronic properties of B-S and H-B-S systems under high pressure

Xin Du,[1] Shoutao Zhang,[1] Jianyan Lin,[1] Xiaohua Zhang,[1] Aitor Bergara,[2,3,4,*] and Guochun Yang[1,†]

[1]*Centre for Advanced Optoelectronic Functional Materials Research and Key Laboratory for UV Light-Emitting Materials and Technology of Northeast Normal University, Changchun 130024, China*

[2]*Departamento de Física de la Materia Condensada, Universidad del País Vasco-Euskal Herriko Unibertsitatea, UPV/EHU, 48080 Bilbao, Spain*

[3]*Donostia International Physics Center (DIPC), 20018 Donostia, Spain*

[4]*Centro de Física de Materiales CFM, Centro Mixto CSIC-UPV/EHU, 20018 Donostia, Spain*

(Received 15 July 2019; revised manuscript received 4 October 2019; published 29 October 2019)

Pressure has become an effective way to obtain new materials with desirable properties. Considering the various stoichiometries, wide applications, and unique structures of binary H-S, H-B, and B-S compounds, especially at high pressures, it is worth expecting that they might form ternary compounds with interesting properties as well. Here, phase stabilities of H-B-S ternary compounds, in the pressure range from 0 to 200 GPa, are reliably determined through first-principles unbiased structural search calculations. A hitherto unknown orthorhombic HBS compound with *Ama*2 symmetry is identified to be stable above 25 GPa, in which B and S atoms alternate to form distorted chains and H atoms are covalently bonded with Bs. With pressure, *Ama*2 HBS undergoes a semiconductor-to-metal electronic transition and even becomes superconducting. The exploration of the binary B-S phase diagram indicates that B-S compounds tend to decompose into elemental solids above 208 GPa. However, two S-rich phases, B_2S_3 and BS_2, are predicted at low pressures, exhibiting semiconducting and metallic properties, respectively. BS_2 shows a calculated T_c value of 21.9 K at 200 GPa, becoming a superconductor among bulk binary B-S compounds.

DOI: 10.1103/PhysRevB.100.134110

I. INTRODUCTION

One of the most important challenges in condensed matter physics and materials science is the prediction of high-temperature superconductors [1,2]. Among the various superconducting materials, high-pressure stable hydrogen-rich compounds have become the main candidates to superconductor at room temperature due to the strong electron-phonon coupling and light atomic mass of hydrogen [3–7]. Recently, the synergy between experimental and theoretical studies has again broken the record of superconducting transition temperatures, reigniting a new wave in the research of H-rich compounds [8–11].

Up to now, most studies were focused on binary hydrides [12–20]. The recent progress on this theme can be found in review articles [21–27]. However, ternary hydrides might also be potential high-temperature superconductors [28–33], and some studies have shown that they not only show high superconducting transition temperatures (T_c) but also exhibit unexpected superconducting mechanisms. For example, the predicted ternary hydride $MgSiH_6$ has a T_c value of 63 K at 250 GPa, and its superconducting transition mainly comes from phonon softenings along $\Gamma \rightarrow X$ and $\Gamma \rightarrow M$ directions [34]. H_6SSe, obtained from H_3S with half of its S atoms replaced by Se, presents a lower T_c value than that of H_3S, indicating that a strong covalent bonding is a dominant factor in these superconducting materials [35]. Pressure-induced stable H_3SXe might also become a high-temperature superconductor, where Xe facilitates the hydrogen-bond symmetrization [36]. Additionally, several ternary hydrides, such as Fe_2SH_3 [37], $BaReH_9$ [38], $KAuH_2$ [39], $CaYH_{12}$ [30], and $MgCH_4$ [40], also show superconductivity.

It is well accepted that pressure favors the stabilization of unusual stoichiometric compounds [41–44], exhibiting interesting physical and chemical properties. For example, several stable sulfur hydrides (e.g., H_2S_3, H_3S_2, HS_2, H_3S, and H_4S_3) [45–47] have been identified at high pressures. More interestingly, H_3S shows a remarkably high T_c value of 203 K [48]. On the other hand, boron (B) and H can form stable binary compounds at both ambient and high pressures. B_2H_6 is a highly reactive and versatile reagent and a high-energy-density material at ambient pressure which metallizes and even becomes a superconductor under high pressure [49–55]. Extensive efforts have been made to investigate their high-pressure phase diagram [56,57]. Thus far, two stable boron hydrides have been found (e.g., BH and BH_2). The semiconducting *Ibam* BH phase transforms into the metallic $P6/mmm$ structure, which also becomes a superconductor with a T_c of $14.1 \sim 21.4$ K at 168 GPa [56]. For B-S compounds, most of the current studies are focused on structures and electronic properties at ambient pressure [58–62]. Structural phase transitions of BS and B_2S_3 have been studied below 50 GPa [63–65]. Thus far, their high-pressure phase diagram with a wide range of chemical compositions has not been fully determined yet.

*Corresponding author: a.bergara@ehu.eus
†Corresponding author: yanggc468@nenu.edu.cn

Considering the rich structures, phase stabilities, and diverse properties of H-S, H-B, and B-S binary systems, it may be worth studying H-B-S ternary compounds under high pressure. In this work, to reliably determine the phase diagram of H-B-S ternary compounds, we first explore the stable B-S compounds with various B_xS_y (x and $y = 1-5$; $x = 1-5$ and $y = 1$; $x = 2-3$ and $y = 3-2$) compositions at high pressures through first-principles swarm-intelligence structural calculations [66,67]. Then, candidate structures of H-B-S ternary compounds with $H_xB_yS_z$ ($x = 1-10$; $y = 1-2$; $z = 1-2$) compositions are considered to build the ternary phase diagram. There is just one stable chemical composition in H-B-S under high pressure. The semiconducting orthorhombic HBS is found to be stable at 25 GPa, which becomes metallic at ∼200 GPa and appears to be superconducting at 300 GPa. Stable binary B-S compounds become unstable with respect to elemental solids at very high pressures. Interestingly, the newly identified BS_2 compound becomes a superconductor with a T_c of 21.9 K at 200 GPa. Our work provides an opportunity to understand the structures and properties of H-B-S and B-S systems at high pressures.

II. COMPUTATIONAL DETAILS

First-principles-based structural prediction technology plays an important role in the discovery of new materials, especially at high pressures [66,68–70]. In order to reliably determine the phase stability, finding adequate candidates is a necessary prerequisite. Our structure searches of H-B-S and B-S systems were performed with the CALYPSO prediction method based on swarm intelligence [67]. CALYPSO is able to find the most stable structure by just knowing the chemical composition, whose effectiveness has been confirmed in various kinds of compounds [37,45,71–74]. Specific details of the calculations are given in the Supplemental Material [75].

Calculations of the structural relaxations and electronic properties were carried out using density functional theory (DFT) [76,77] as implemented in the Vienna ab initio Simulation Package (VASP) code [78]. The exchange-correlation energy was treated within the Perdew-Burke-Ernzerhof (PBE) [79] generalized gradient approximation (GGA) [80]. The adopted all-electron projector augmented-wave (PAW) [81] pseudopotentials of B, S, and H treat $2s^2\,2p^1$, $3s^2\,3p^4$, and $1s^1$ electrons as the valence electrons. To obtain a better energy convergence, we have chosen a plane-wave cutoff energy of 800 eV and Monkhorst-Pack k meshes [82] of $2\pi \times 0.03\,\text{Å}^{-1}$. Phonon dispersion calculations, as implemented in the PHONOPY code [83], were used to determine the dynamic stability of thermodynamically stable phases. The electron-phonon coupling for superconducting properties of stable metal phases are performed within the framework of the linear-response theory via the Quantum ESPRESSO package [84].

III. RESULTS AND DISCUSSION

A. Phase stability

To reliably determine the phase stability of ternary compounds at high pressures, we need to know the stable structures of the corresponding binary compounds or elemental solids. As discussed above, the high-pressure phase diagrams of binary B-H and S-H compounds have been extensively studied, but the binary phase stability of B-S compounds at high pressures has not been explored. First, we perform an extensive structure search to find the most stable structures for each B_xS_y ($x = 1$ and $y = 1-5$; $x = 1-5$ and $y = 1$; $x = 2-3$ and $y = 3-2$) composition at 0 K and selected pressures of 1 atm and 25, 50, 100, and 200 GPa via first-principles swarm-intelligence search calculations. The calculated convex hull is shown in Fig. S1 (see Supplemental Material [75]). Besides reproducing the already known structures, we find another two S-rich phases of B_2S_3 and BS_2. Notably, B-S compounds, stabilized at atmospheric and low pressures, tend to decompose with respect to elemental solids above 208 GPa.

Considering that H-rich compounds might show high superconducting transition temperatures, we have mainly focused in the structural prediction of H-rich compositions of $H_xB_yS_z$ ($x = 1-10$; $y = 1-2$; $z = 1-2$) at 25, 50, 100, and 200 GPa. Then, we have chosen the structure with the

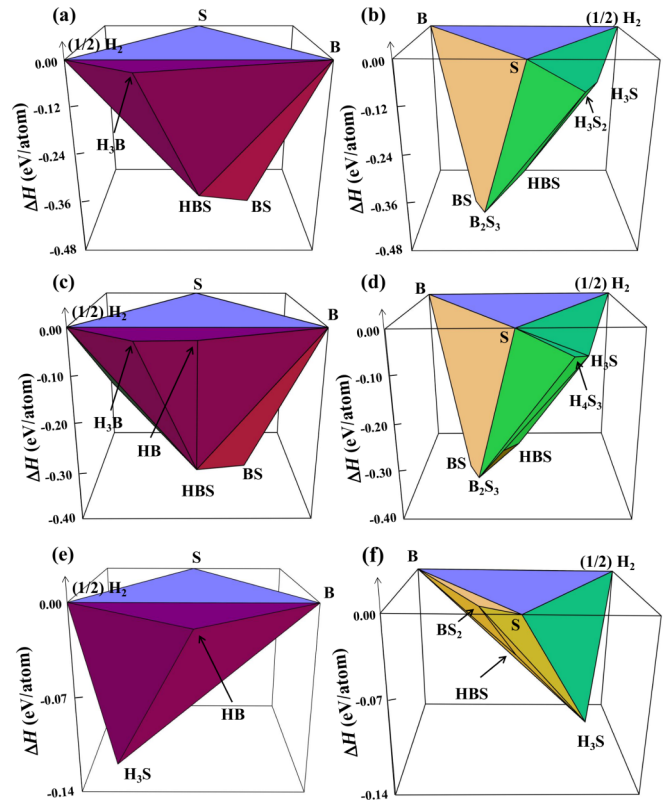

FIG. 1. Phase diagram of H-B-S system at (a), (b) 25 GPa, (c), (d) 50 GPa, and (e), (f) 200 GPa. At 25 GPa, P-1 H_3B [50], $C2/c$ H_3S [46], $P2_1$ H_3S_2 [47], R-3m BS [57], Cc B_2S_3, $P6_3/m$ (1/2) H_2 [86], $Pnnm$ for B [87], and $I4_1/acd$ for S [88] are used to determine the phase stability. On the other hand, at 50 GPa, $Ibam$ HB, $P2_1/c$ H_3B [56], $C2/c$ H_3S [46], $P2_12_12_1$ H_4S_3 [46], Cc B_2S_3, P-3m1 BS [64], $P6_3/m$ for (1/2) H_2, $Pnnm$ for B [56], and $I4_1/acd$ for S [88] are chosen. Finally, at 200 GPa, $P6/mmm$ HB [56], Im-3m H_3S [46], $C2/c$ for (1/2) H_2, $Cmca$ for B [56], and R-3m for S [89] are selected.

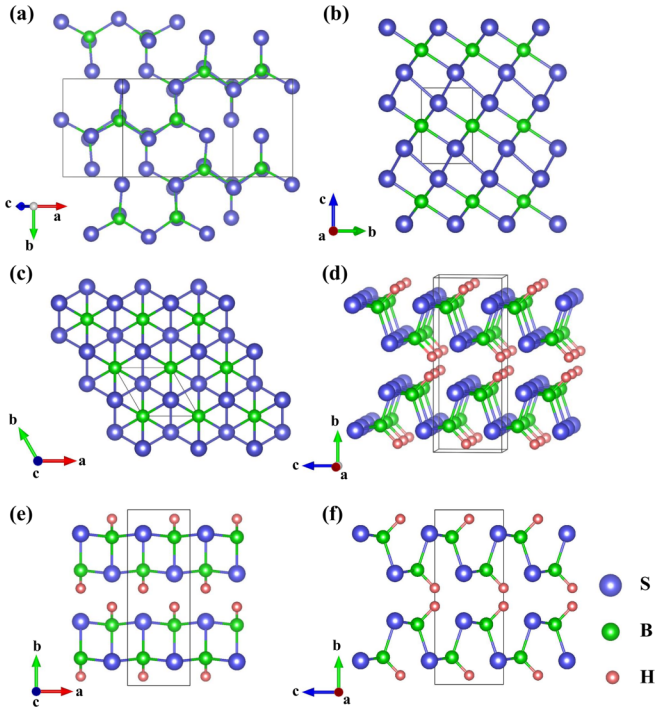

FIG. 2. Crystal structures of the stable compounds: (a) *Cc* B_2S_3 at 50 GPa, (b), (c) *P*-3*m*1 BS_2 at 200 GPa, and (d), (e), (f) *Ama*2 HBS at 100 GPa. Pink, green, and purple spheres represent H, B, and S atoms, respectively.

lower enthalpy to determine the relative phase stability. In general, for ternary compounds, the structure with a negative formation enthalpy with respect to binary compounds, elemental solids, or their combinations becomes a potential candidate for experimental synthesis. The calculated convex hulls for H-B-S compounds are shown in Fig. 1, where the phases located at the edges of the polyhedron are thermodynamically stable [85]. In the pressure range we are considering, HBS is the only stable ternary compound. The absence of any imaginary frequencies in the calculated phonon dispersion curves of *Cc* B_2S_3, *P*-3*m*1 BS_2, and *Ama*2 HBS indicate they are dynamically stable (Fig. S2 [75]).

B. Structural geometry

Previous studies found two stable phases for B_2S_3 [61,63] with $P2_1/c$ and $I4_1/a$ symmetries. However, according to our structural predictions, another B_2S_3 phase [space group *Cc,* four formula units per cell; Fig. 2(a)] becomes stable above 15 GPa. In *Cc* B_2S_3 each B atom is four-coordinated, whereas S atoms have two different coordination environments: one is two-coordinated while the other is three-coordinated. The basic building block is a B_3S_3 six-membered ring with an alternated arrangement of B and S atoms, which has also been observed in the other two low-pressure phases (Fig. S3 [75]). *Cc* B_2S_3 decomposes into BS and S above 95 GPa (Fig. S4 [75]). $P2_1/c$ BS_2 is already stable at ambient pressure [58] but decomposes with pressure (Fig. S5 [75]). However, according to our structural search, BS_2 becomes stable again at the pressure range of 170 ∼ 208 GPa [space group *P*-3*m*1, 1 formula unit per cell; Figs. 2(b) and 2(c)]. In *P*-3*m*1 BS_2 each B atom is six-coordinated with S atoms, whereas S atoms are three-coordinated both with B and S, forming an interconnected zigzaglike S atom layer with an S-S distance of 2.06 Å, which is shorter than S_2^{2-}(2.12 Å) in Li_2S_2 [90]. HBS stabilizes into an orthorhombic structure [space group *Ama*2, four formula units per cell; Fig. 2(d)] and has no phase transitions in the considered pressure range. The most striking feature is that B and S atoms alternate to form a distorted chain along the *c* direction, in which H atoms attach to B atoms. These chains are crosslinked through B-S bonds in the *ac* plane, showing a typical layered structure. Moreover, the above-mentioned alternated arrangement of B_3S_3 six-membered rings is also observed.

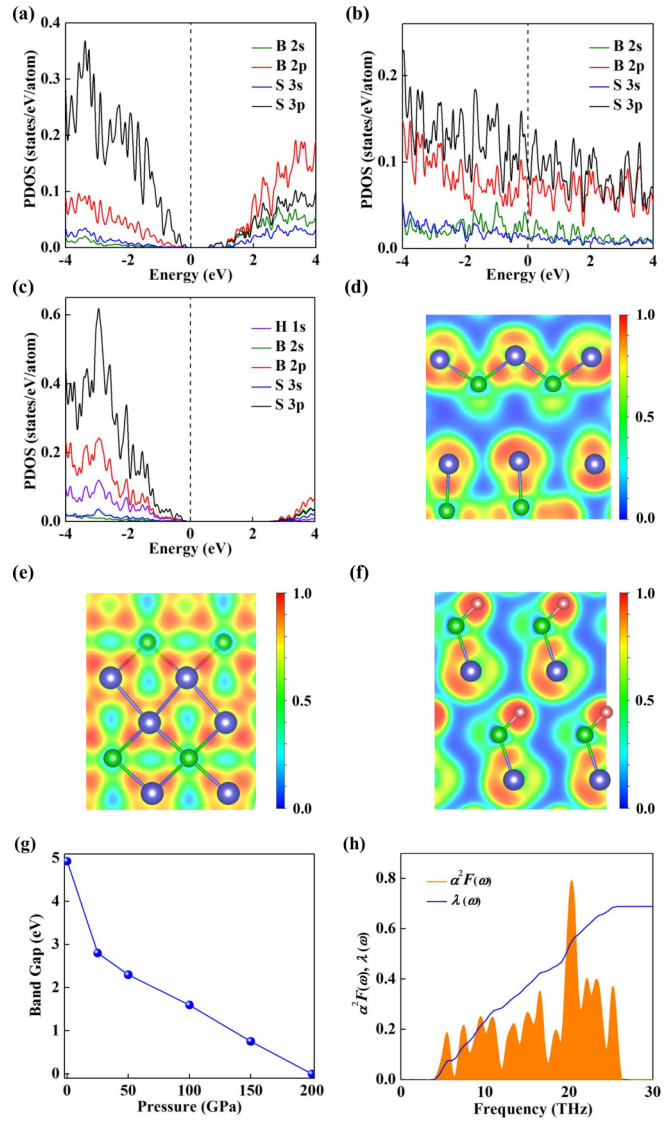

FIG. 3. Projected density of states (PDOS) within the HSE06 hybrid functional of (a) *Cc* B_2S_3, (b) *P*-3*m*1 BS_2, and (c) *Ama*2 HBS at 50, 200, and 25 GPa, respectively. The vertical dashed line represents the Fermi level. (d), (e), (f) The ELF of B_2S_3, BS_2, and HBS, respectively. (g) The calculated band gap of *Ama*2 HBS as a function of pressure from 0 to 200 GPa. (h) The Eliashberg spectral function $\alpha^2F(\omega)$ and integrated electron-phonon coupling parameters $\lambda(\omega)$ of *P*-3*m*1 BS_2 at 200 GPa.

C. Electronic properties

To reliably determine the electronic properties, we have chosen the Heyd-Scuseria-Ernzerhof (HSE06) [91,92] hybrid functional to calculate the electronic band structures and partial density of states (PDOS) of B_2S_3, BS_2, and HBS [Fig. S6 [75] and Figs. 3(a)–3(c)]. Both B_2S_3 and HBS show indirect-band-gap semiconducting character with band-gap values of 0.8 and 2.8 eV, respectively, whereas BS_2 is metallic. For B_2S_3 and BS_2, there is a strong overlap between S $2p$ and B $2p$ orbitals below the Fermi level [Figs. 3(a) and 3(b)], indicating the formation of a strong chemical bonding. For BS_2, the flatband analysis shows that the S $3p$ orbital makes the major contribution to the Fermi level (Fig. S7 [75]). The analysis of the electronic localization function (ELF) [93] further confirms that B-S and S-S bonds are covalent [Figs. 3(d) and 3(e)]. Bader charge analysis shows charge transfer from B to S, indicating that B-S bonds are polar covalent (Table S2 [75]) [94]. The PDOS of HBS exhibits there is a strong hybridization between S $2p$ and B $2p$, and H $1s$ and B $2p$ or $2s$ states [Fig. 3(c)], which are also covalent bondings [Fig. 3(f)]. The pressure-dependent electronic properties show the band gap of HBS gradually decreases and eventually closes, becoming a metal at 200 GPa [Fig. 3(g)].

Considering the already known superconductivity of binary H-S and H-B compounds and the pressure-induced metallization of BS_2 and HBS, we have also explored their eventual superconducting transitions. Surprisingly, the calculated superconducting transition temperature (T_c) of BS_2 is 21.9 K at 200 GPa, which is higher than 9.3 K of HS_2 [47]. The analysis of the projected phonon density of states indicates that frequency vibrations mainly originate from the coupling between B and S atoms (Fig. S8 [75]). The integrated electron-phonon coupling parameter $\lambda(\omega)$ and Eliashberg spectral function $\alpha^2F(\omega)$ are shown in Fig. 3(h). The calculated λ is 0.69 at 200 GPa and is much lower than the 2.19 of H_3S [95]. For HBS, it shows no superconductivity at 200 GPa but becomes superconducting at 300 and 400 GPa with T_c of 0.8 and 1.9 K, respectively. The analysis of the projected phonon density of states indicates that the low-frequency vibrations ($<$15 THz) mainly originate from the coupling between B and S atoms; the high-frequency modes are associated with H atoms, while the middle-frequency stretching modes come from the coupling between B and H (Fig. S8 [75]). The integrated electron-phonon coupling parameter $\lambda(\omega)$ and Eliashberg spectral function $\alpha^2F(\omega)$ are shown in Fig. S8 [75]. The calculated λ is only 0.27 at 300 GPa, and the low-frequency translational vibration ($<$42 THz) modes give the main contribution (95%) to λ.

IV. CONCLUSIONS

In summary, high-pressure phase diagrams of B-S and H-B-S systems are reliably built through first-principles swarm-intelligence structural search calculations. A semiconducting B_2S_3 phase is identified above 15 GPa. The identified $P\text{-}3m1$ BS_2 compound is a superconductor in the bulk binary B-S compounds, having a T_c of 21.9 K at 200 GPa. For ternary H-B-S systems, the only stable compound under pressure is HBS, exhibiting diverse pressure-related electronic properties (i.e., semiconductor $\rightarrow$ metallizatic $\rightarrow$ superconductor). Chemical bonding analysis reveals that the structural stability of HBS and B-S compounds is mainly attributed to the strong B-S covalent bonds.

ACKNOWLEDGMENTS

The authors acknowledge funding support from the Natural Science Foundation of China under Grants No. 21573037, No. 21873017, No. 11704062, and No. 51732003, the Postdoctoral Science Foundation of China under Grant No. 2013M541283, the Natural Science Foundation of Jilin Province (Grant No. 20190201231JC), the "111" Project (No. B13013), and the Fundamental Research Funds for the Central Universities (2412017QD006). The work was carried out at National Supercomputer Center in Tianjin, and the calculations were performed on TianHe-1 (A). A.B. acknowledges financial support from the Spanish Ministry of Economy and Competitiveness (FIS2016-76617-P) and the Department of Education, Universities and Research of the Basque Government and the University of the Basque Country (IT756-13).

[1] H. Wang, X. Li, G. Gao, Y. Li, and Y. Ma, Wiley Interdiscip. Rev.: Comput. Mol. Sci. **8**, e1330 (2018).
[2] H.-K. Mao, X.-J. Chen, Y. Ding, B. Li, and L. Wang, Rev. Mod. Phys. **90**, 015007 (2018).
[3] J. S. Tse, Y. Yao, and K. Tanaka, Phys. Rev. Lett. **98**, 117004 (2007).
[4] A. Shamp, T. Terpstra, T. Bi, Z. Falls, P. Avery, and E. Zurek, J. Am. Chem. Soc. **138**, 1884 (2016).
[5] V. V. Struzhkin, D. Y. Kim, E. Stavrou, T. Muramatsu, H.-k. Mao, C. J. Pickard, R. J. Needs, V. B. Prakapenka, and A. F. Goncharov, Nat. Commun. **7**, 12267 (2016).
[6] X.-J. Chen, J.-L. Wang, V. V. Struzhkin, H.-k. Mao, R. J. Hemley, and H.-Q. Lin, Phys. Rev. Lett. **101**, 077002 (2008).
[7] Y. Li, G. Gao, Y. Xie, Y. Ma, T. Cui, and G. Zou, Proc. Natl. Acad. Sci. USA **107**, 15708 (2010).
[8] H. Liu, I. I. Naumov, R. Hoffmann, N. W. Ashcroft, and R. J. Hemley, Proc. Natl. Acad. Sci. USA **114**, 6990 (2017).
[9] F. Peng, Y. Sun, C. J. Pickard, R. J. Needs, Q. Wu, and Y. Ma, Phys. Rev. Lett. **119**, 107001 (2017).
[10] A. P. Drozdov, P. P. Kong, V. S. Minkov, S. P. Besedin, M. A. Kuzovnikov, S. Mozaffari, L. Balicas, F. F. Balakirev, D. E. Graf, V. B. Prakapenka *et al.*, Nature (London) **569**, 528 (2019).
[11] M. Somayazulu, M. Ahart, A. K. Mishra, Z. M. Geballe, M. Baldini, Y. Meng, V. V. Struzhkin, and R. J. Hemley, Phys. Rev. Lett. **122**, 027001 (2019).
[12] E. S. Wiedner, M. B. Chambers, C. L. Pitman, R. M. Bullock, A. J. M. Miller, and A. M. Appel, Chem. Rev. **116**, 8655 (2016).
[13] K. Abe, Phys. Rev. B **96**, 144108 (2017).

[14] T. Scheler, M. Marqués, Z. Konôpková, C. L. Guillaume, R. T. Howie, and E. Gregoryanz, Phys. Rev. Lett. **111**, 215503 (2013).

[15] B. Li, Y. Ding, D. Y. Kim, R. Ahuja, G. Zou, and H.-K. Mao, Proc. Natl. Acad. Sci. USA **108**, 18618 (2011).

[16] J. Ying, X. Li, E. Greenberg, V. B. Prakapenka, H. Liu, and V. V. Struzhkin, Phys. Rev. B **99**, 224504 (2019).

[17] T. Scheler, F. Peng, C. L. Guillaume, R. T. Howie, Y. Ma, and E. Gregoryanz, Phys. Rev. B **87**, 184117 (2013).

[18] G. Gao, R. Hoffmann, N. W. Ashcroft, H. Liu, A. Bergara, and Y. Ma, Phys. Rev. B **88**, 184104 (2013).

[19] S. Yu, X. Jia, G. Frapper, D. Li, A. R. Oganov, Q. Zeng, and L. Zhang, Sci. Rep. **5**, 17764 (2015).

[20] M. A. Kuzovnikov and M. Tkacz, Phys. Rev. B **93**, 064103 (2016).

[21] E. Zurek and T. Bi, J. Chem. Phys. **150**, 050901 (2019).

[22] E. Zurek, Comments Inorg. Chem. **37**, 78 (2017).

[23] H.-Y. Lv, M. Chen, Y. Feng, W.-J. Li, G.-H. Zhong, and C.-L. Yang, J. Chin. Chem. Soc. **66**, 1246 (2019).

[24] D. Duan, Y. Liu, Y. Ma, Z. Shao, B. Liu, and T. Cui, Natl. Sci. Rev. **4**, 121 (2017).

[25] J. A. Flores-Livas, L. Boeri, A. Sanna, G. Profeta, R. Arita, and M. Eremets, arXiv:1905.06693.

[26] T. Bi, N. Zarifi, T. Terpstra, and E. Zurek, Reference Module in Chemistry, Molecular Sciences and Chemical Engineering (2019), doi: 10.1016/B978-0-12-409547-2.11435-0.

[27] D. V. Semenok, I. A. Kruglov, I. A. Savkin, A. G. Kvashnin, and A. R. Oganov, arXiv:1806.00865.

[28] M. A. Olea-Amezcua, O. De la Peña-Seaman, and R. Heid, Phys. Rev. B **99**, 214504 (2019).

[29] C. Zhang, G. Sun, J. Wang, C. Lu, Y. Jin, X. Kuang, and A. Hermann, ACS Appl. Mater. Interfaces **9**, 26169 (2017).

[30] X. Liang, A. Bergara, L. Wang, B. Wen, Z. Zhao, X.-F. Zhou, J. He, G. Gao, and Y. Tian, Phys. Rev. B **99**, 100505(R) (2019).

[31] D. Meng, M. Sakata, K. Shimizu, Y. Iijima, H. Saitoh, T. Sato, S. Takagi, and S.-i. Orimo, Phys. Rev. B **99**, 024508 (2019).

[32] Y. Ma, D. Duan, Z. Shao, D. Li, L. Wang, H. Yu, F. Tian, H. Xie, B. Liu, and T. Cui, Phys. Chem. Chem. Phys. **19**, 27406 (2017).

[33] Y. Sun, J. Lv, Y. Xie, H. Liu, and Y. Ma, Phys. Rev. Lett. **123**, 097001 (2019).

[34] Y. Ma, D. Duan, Z. Shao, H. Yu, H. Liu, F. Tian, X. Huang, D. Li, B. Liu, and T. Cui, Phys. Rev. B **96**, 144518 (2017).

[35] B. Liu, W. Cui, J. Shi, L. Zhu, J. Chen, S. Lin, R. Su, J. Ma, K. Yang, M. Xu *et al.*, Phys. Rev. B **98**, 174101 (2018).

[36] D. Li, Y. Liu, F.-B. Tian, S.-L. Wei, Z. Liu, D.-F. Duan, B.-B. Liu, and T. Cui, Frontiers Phys. **13**, 137107 (2018).

[37] S. Zhang, L. Zhu, H. Liu, and G. Yang, Inorg. Chem. **55**, 11434 (2016).

[38] T. Muramatsu, W. K. Wanene, M. Somayazulu, E. Vinitsky, D. Chandra, T. A. Strobel, V. V. Struzhkin, and R. J. Hemley, J. Phys. Chem. C **119**, 18007 (2015).

[39] M. Rahm, R. Hoffmann, and N. W. Ashcroft, J. Am. Chem. Soc. **139**, 8740 (2017).

[40] F. Tian, D. Li, D. Duan, X. Sha, Y. Liu, T. Yang, B. Liu, and T. Cui, Mater. Res. Express **2**, 046001 (2015).

[41] M.-s. Miao, X.-l. Wang, J. Brgoch, F. Spera, M. G. Jackson, G. Kresse, and H.-q. Lin, J. Am. Chem. Soc. **137**, 14122 (2015).

[42] J. Lin, S. Zhang, W. Guan, G. Yang, and Y. Ma, J. Am. Chem. Soc. **140**, 9545 (2018).

[43] J. Botana, X. Wang, C. Hou, D. Yan, H. Lin, Y. Ma, and M.-s. Miao, Angew. Chem. Int. Ed. **54**, 9280 (2015).

[44] J. Lin, Z. Zhao, C. Liu, J. Zhang, X. Du, G. Yang, and Y. Ma, J. Am. Chem. Soc. **141**, 5409 (2019).

[45] Y. Li, J. Hao, H. Liu, Y. Li, and Y. Ma, J. Chem. Phys. **140**, 174712 (2014).

[46] Y. Li, L. Wang, H. Liu, Y. Zhang, J. Hao, C. J. Pickard, J. R. Nelson, R. J. Needs, W. Li, Y. Huang *et al.*, Phys. Rev. B **93**, 020103(R) (2016).

[47] I. Kruglov, R. Akashi, S. Yoshikawa, A. R. Oganov, and M. M. D. Esfahani, Phys. Rev. B **96**, 220101(R) (2017).

[48] A. P. Drozdov, M. I. Eremets, I. A. Troyan, V. Ksenofontov, and S. I. Shylin, Nature (London) **525**, 73 (2015).

[49] K. Abe and N. W. Ashcroft, Phys. Rev. B **84**, 104118 (2011).

[50] Y. Yao and R. Hoffmann, J. Am. Chem. Soc. **133**, 21002 (2011).

[51] A. M. Murcia Rios, D. N. Komsa, and V. N. Staroverov, J. Phys. Chem. C **122**, 14781 (2018).

[52] C. Murli and Y. Song, J. Phys. Chem. B **113**, 13509 (2009).

[53] A. Torabi, Y. Song, and V. N. Staroverov, J. Phys. Chem. C **117**, 2210 (2013).

[54] A. Torabi, C. Murli, Y. Song, and V. N. Staroverov, Sci. Rep. **5**, 13929 (2015).

[55] Y. Song, C. Murli, and Z. Liu, J. Chem. Phys. **131**, 174506 (2009).

[56] C.-H. Hu, A. R. Oganov, Q. Zhu, G.-R. Qian, G. Frapper, A. O. Lyakhov, and H.-Y. Zhou, Phys. Rev. Lett. **110**, 165504 (2013).

[57] W.-H. Yang, W.-C. Lu, S.-D. Li, X.-Y. Xue, Q.-J. Zang, K. M. Ho, and C. Z. Wang, Phys. Chem. Chem. Phys. **21**, 5466 (2019).

[58] B. Krebs and H.-U. Hürter, Angew. Chem. **92**, 479 (1980).

[59] H. Wu, X. Li, R. Zhang, and J. Yang, J. Mater. Chem. A **7**, 3752 (2019).

[60] B. Mortazavi and T. Rabczuk, Energies **11**, 1573 (2018).

[61] H. Diercks and B. Krebs, Angew. Chem., Int. Ed. Engl. **16**, 313 (1977).

[62] D. Fan, C. Yang, S. Lu, and X. Hu, arXiv:1803.03459.

[63] T. Sasaki, H. Takizawa, K. Uheda, T. Yamashita, and T. Endo, J. Solid State Chem. **166**, 164 (2002).

[64] K. A. Cherednichenko, I. A. Kruglov, A. R. Oganov, Y. Le Godec, M. Mezouar, and V. L. Solozhenko, J. Appl. Phys. **123**, 135903 (2018).

[65] T. Sasaki, H. Takizawa, K. Uheda, and T. Endo, Phys. Status Solidi B **223**, 29 (2001).

[66] Y. Wang, J. Lv, L. Zhu, and Y. Ma, Phys. Rev. B **82**, 094116 (2010).

[67] Y. Wang, J. Lv, L. Zhu, and Y. Ma, Comput. Phys. Commun. **183**, 2063 (2012).

[68] A. R. Oganov and C. W. Glass, J. Chem. Phys. **124**, 244704 (2006).

[69] C. J. Pickard and R. J. Needs, J. Phys.: Condens. Matter **23**, 053201 (2011).

[70] S. Curtarolo, G. L. W. Hart, M. B. Nardelli, N. Mingo, S. Sanvito, and O. Levy, Nat. Mater. **12**, 191 (2013).

[71] L. Zhang, Y. Wang, J. Lv, and Y. Ma, Nat. Rev. Mater. **2**, 17005 (2017).

[72] J. Lv, Y. Wang, L. Zhu, and Y. Ma, Phys. Rev. Lett. **106**, 015503 (2011).

[73] L. Zhu, H. Wang, Y. Wang, J. Lv, Y. Ma, Q. Cui, Y. Ma, and G. Zou, Phys. Rev. Lett. **106**, 145501 (2011).

[74] H. Wang, J. S. Tse, K. Tanaka, T. Iitaka, and Y. Ma, Proc. Natl. Acad. Sci. USA **109**, 6463 (2012).

[75] See Supplemental Material at http://link.aps.org/supplemental/10.1103/PhysRevB.100.134110 for computational details, the convex hull of B-S system between 1 atm to 200 GPa, structural information, phonon dispersion curves, electronic properties, superconductive properties, and Bader charge analysis of B-S phases.
[76] P. Hohenberg and W. Kohn, Phys. Rev. **136**, B864 (1964).
[77] W. Kohn and L. J. Sham, Phys. Rev. **140**, A1133 (1965).
[78] G. Kresse and J. Furthmüller, Phys. Rev. B **54**, 11169 (1996).
[79] J. P. Perdew, K. Burke, and M. Ernzerhof, Phys. Rev. Lett. **77**, 3865 (1996).
[80] J. P. Perdew, J. A. Chevary, S. H. Vosko, K. A. Jackson, M. R. Pederson, D. J. Singh, and C. Fiolhais, Phys. Rev. B **46**, 6671 (1992).
[81] P. E. Blöchl, Phys. Rev. B **50**, 17953 (1994).
[82] H. J. Monkhorst and J. D. Pack, Phys. Rev. B **13**, 5188 (1976).
[83] A. Togo, F. Oba, and I. Tanaka, Phys. Rev. B **78**, 134106 (2008).
[84] P. Giannozzi, S. Baroni, N. Bonini, M. Calandra, R. Car, C. Cavazzoni, D. Ceresoli, G. L Chiarotti, M. Cococcioni, I. Dabo *et al.*, J. Phys.: Condens. Matter **21**, 395502 (2009).
[85] L. Zhu, H. Liu, R. E. Cohen, R. Hoffmann, and T. A. Strobel, arXiv:1708.03483.
[86] C. J. Pickard and R. J. Needs, Nat. Phys. **3**, 473 (2007).
[87] A. R. Oganov, J. Chen, C. Gatti, Y. Ma, Y. Ma, C. W. Glass, Z. Liu, T. Yu, O. O. Kurakevych, and V. L. Solozhenko, Nature (London) **457**, 863 (2009).
[88] Y. Akahama, M. Kobayashi, and H. Kawamura, Phys. Rev. B **48**, 6862 (1993).
[89] H. Luo, R. G. Greene, and A. L. Ruoff, Phys. Rev. Lett. **71**, 2943 (1993).
[90] G. Yang, S. Shi, J. Yang, and Y. Ma, J. Mater. Chem. A **3**, 8865 (2015).
[91] J. Heyd, G. E. Scuseria, and M. Ernzerhof, J. Chem. Phys. **118**, 8207 (2003).
[92] A. V. Krukau, O. A. Vydrov, A. F. Izmaylov, and G. E. Scuseria, J. Chem. Phys. **125**, 224106 (2006).
[93] A. D. Becke and K. E. Edgecombe, J. Chem. Phys. **92**, 5397 (1990).
[94] R. F. W. Bader, Acc. Chem. Res. **18**, 9 (1985).
[95] D. Duan, Y. Liu, F. Tian, D. Li, X. Huang, Z. Zhao, H. Yu, B. Liu, W. Tian, and T. Cui, Sci. Rep. **4**, 6968 (2014).